Neuropsychiatric Disease and Treatment Dovepress

Open Access Full Text Article ORIGINAL RESEARCH

Shisandra Decoction Alleviates Parkinson's Disease Symptoms in a Mouse Model Through PI3K/AKT/mTOR Signalling Pathway

Yawen Pan[1], Mojinzi Chen[2], Lulu Pan[3], Qiuling Tong[4], Zhiqing Cheng[3], Sujin Lin[3], Rongrong Pan[3], Mengyuan Chen[1], Yinghao Zhi[3]

[1]Wenzhou TCM Hospital of Zhejiang Chinese Medical University, Wenzhou, 325000, People's Republic of China; [2]Physician,Wenzhou Hospital of Integrated Traditional Chinese and Western Medicine, Wenzhou, 325000, People's Republic of China; [3]Department of Rehabilitation Medicine, Wenzhou TCM Hospital of Zhejiang Chinese Medical University, Wenzhou, 325000, People's Republic of China; [4]The First Affiliated Hospital of Wenzhou Medical University, Wenzhou, 325000, People's Republic of China

Correspondence: Yinghao Zhi, Department of Rehabilitation Medicine, Wenzhou TCM Hospital of Zhejiang Chinese Medical University, Wenzhou, 325000, People's Republic of China, Tel +86-13758472924, Email 43914515@qq.com

Purpose: The present study aimed to characterize neuroprotective effects of Schisandra Decoction (Sch D) treatment in a mouse model of Parkinson's disease (PD), and to explore underlying mechanisms focused on the mammalian target of rapamycin (mTOR) signaling pathway.

Materials and Methods: 50 male C57 BL/6 mice were randomly assigned to either control (n = 10) or 1-methyl-4-phenyl-1,2,3,6-tetrahydropyridine (MPTP) model (n = 40) groups. PD mice were further divided into four groups of ten mice each: MPTP group, LY294002 group, Sch D group, and LY2940002 + Sch D group. Mice from each group were assessed in pole climbing, rotary rod and open field tests. Brain Tyrosine hydroxylase (TH) protein was observed using immunohistochemistry. mRNA levels of PTEN, PI3K and LC3 in brain tissue were measured using RT-PCR. Protein levels of PTEN, PI3K, Akt, p-Akt, mTOR, p-mTOR, p70s6K, p62, LC3II / I, α-synuclein (α-syn), TH in brain tissue were assessed by Western blotting (WB).

Results: In behavioral tests, PD mice treated with Sch D showed reduced pole climbing time, longer rotarod duration, and greater distance traveled. In terms of neuroprotection, PD mice in the Sch D group exhibited higher levels of TH protein and enhanced α-syn clearance. Regarding autophagy, compared to the control group, mice in the MPTP group had elevated PTEN protein expression, which inhibited PI3K, p-AKT/AKT, and p-mTOR/mTOR protein levels, decreased LC3II/I protein expression, and increased P62 protein expression. Treatment with Sch D reversed these effects.

Conclusion: Sch D reduces α-syn aggregation in the brains of MPTP-induced PD model mice, exerts neuroprotective effects, and improves motor function. Additionally, Sch D inhibits autophagy through the PI3K/AKT/mTOR pathway. The neuroprotective effect of Sch D may involve the suppression of abnormal autophagy and its antioxidant properties, which indirectly reduces α-syn accumulation. Future studies should assess the impact of Sch D on oxidative stress markers to evaluate its antioxidant effects.

Keywords: Parkinson's disease, Shisandra decoction, mTOR signaling pathway, autophagy, traditional Chinese medicine

Introduction

Parkinson's disease (PD), the second-most prevalent degenerative neurological disease, affects approximately 6 million individuals globally.[1] The incidence of PD is furthermore increasing with increased aging of populations. Prevalent clinical symptoms include static tremors, stiffness, bradykinesia, postural gait issues and other motor abnormalities. Non-motor symptoms include decreased mental functioning, autonomic issues, and sensory disturbances.[2] PD dramatically reduces patients' daily quality of life. The disease is characterized by an exceptionally complex pathophysiology, the cardinal hallmark of which is loss of dopaminergic neurons in the substantia nigra. Lewy bodies, neuronal inclusions mainly constituted of aggregates of the neurotransmitter α-synuclein (α-syn), are characteristic pathological features.[3]

Received: 7 May 2024
Accepted: 28 September 2024
Published: 23 October 2024

The multiplication of SNCA loci leading to elevated α-syn levels is directly correlated with PD progression,[4] and reducing α-syn levels add potential therapeutic strategy for improving PD symptoms.

Abnormal abundance of α-syn protein inhibits autophagy in neurons by altering the trafficking of autophagy-related proteins (eg ATG9) between the endoplasmic reticulum and the Golgi complex, along with decreasing the production of autophagosomal precursors.[5] Autophagy begins with the formation of nascent autophagosomal vacuoles or isolation membranes. Normally, under conditions of nutrient limitation, Adenosine 5′-monophosphate -activated protein kinase (AMPK) activation and mTOR inhibition together activate Unc-51-like kinases (ULK), which in turn activates the VPS34 complex and induces the formation of isolation membranes that ultimately result in the formation of autophagosomes. The latter undergoes amalgamation with lysosomes, enabling catabolism of cytoplasmic cellular constituents.[6] Autophagy is a critical mechanism for the removal of protein aggregates observed in multiple neuronal diseases and perturbations in the autophagic process are known to be associated with degenerative neuropathies.[7]

Autophagy is normally regulated by multiple signaling pathways, among which the PI3K/AKT/mTOR pathway plays a particularly important role.[8] mTOR is an integral regulatory factor in many neural processes, and loss of mTOR pathway proteins is known to cause early neuronal death during brain development.[9] Because autophagic dysfunction and neurodegeneration are known to be linked, it has been suggested that mTOR activity may significantly affect neurodegenerative disease pathology.[10] Therefore, modulating the process of autophagy by targeting the mTOR signaling pathway, thereby reducing α-syn aggregate abundance, might be a strategy for treating PD.

In clinical studies, traditional Chinese medicines have shown efficacy in relieving PD symptoms as well as improving adverse consequences of long-term use of Western medicines.[11,12] In preclinical investigations, ginsenoside improved motor function in a mouse model of PD by regulating the expression and antioxidant capacity of glutathione (GSH) cysteine ligase.[13] Puerarin increased GSH synthesis in PC12 cells and reduced oxidative stress levels in PD-derived cells.[14] Therefore, research on important monomers and compound formulations has certain value in the treatment of PD. Schisandra Decoction (Sch D), including the following components as shown in Table 1. Based on traditional Chinese medicine principles and years of clinical experience, the famous Traditional Chinese Medicine in Zhejiang Province of our hospital, proposed that nourishing the essence and enriching the marrow is the fundamental therapeutic method PD. The application of Sch D in the treatment of PD has achieved favorable clinical results. It is known for its effect of nourishing essence and enriching marrow. The principal herb in Sch D is schisandra, which is the dried mature fruit of the magnolia vine, a plant of the chisandraceae family. According to the classic book "Shennong Ben Cao Jing", schisandra has a sour and warm nature and possesses functions such as nourishing the kidneys, securing the essence, and calming the mind. In our previous research,[15] we found that Schisandrin A has a protective effect on dopaminergic neurons in the substantia nigra compacta of mice with MPTP-induced Parkinson's disease. When exploring the mechanism of its neuroprotective effect further, we used immunoblotting to find that in the Schisandrin A intervention group, the expression levels of LC3-II, Beclin1, Parkin, and PINK1 in the midbrain of mice were significantly increased, and mTOR phosphorylation was inhibited. However, the effects of Sch D with schisandra as the principal herb, on the expression of phosphorylated substrate p70s6K, autophagic substrate p62/SQSTM1, α-synuclein, and TH are currently unclear. We speculate that the clinically effective Sch D may exert its therapeutic effect on PD through the regulation of

Table 1 Components of the Sch D

Full Botanical Plant Name	Family	English Name	Chinese Name	Grams, g	Used Part
Schisandra repanda (Siebold & Zucc.) Radlk.	Schisandraceae	Schisandra	Wuweizi	15 g	Fruit
Ophiopogon bodinieri H.Lév.	Asparagaceae	Ophiopogon	Maidong	15 g	Tuber
Panax bipinnatifidus var. angustifolius (Burkill) J.Wen	Araliaceae	Panax	Shengshaishen	6 g	Root
Cistanche deserticola Ma	Orobanchaceae	Cistanche	Roucongrong	15 g	Stem
Cuscuta chinensis var. chinensis	Convolvulaceae	Cuscuta	Tusizi	15 g	Seed
Uncaria cordata Merr.	Rubiaceae	Uncaria	Gouteng	20 g	Stem
Zingiber officinale var. officinale	Zingiberaceae	Zingiber	Shengjiang	3 g	Rhizome
Ziziphus jujuba f. lageniformis (Nakai) Kitag.	Rhamnaceae	Ziziphus	Dazao	10 g	Fruit

autophagy. Therefore, this study aims to explore the possible mechanisms of Sch D in the treatment of PD. In this study, we investigated the effect of Sch D on improving motor function in PD mice through behavioral experiments. The expression of TH in the substantia nigra of the mice was measured using immunohistochemistry. Additionally, proteins related to the PI3K/AKT/mTOR pathway and autophagy were examined.

Materials and Methods

Experimental Animals

Healthy male C57BL/6 SPF grade mice aged 6 to 8 weeks (N=50) were purchased from Spafu (Beijing) Biotechnology Co., Ltd. (animal production license number SCXK (Jing) 2019–0010 and animal use license number SYXK (Zhe) 2021–0005). The mice underwent adaptive feeding for 1 week at room temperature (20–24 °C) and 45–65% humidity. All mice were fed and watered *ad libitum*. All animal experimental protocols were approved by the Experimental Animal Ethics Council of Zhejiang Haikang Biological Product Co., Ltd. (approval code HKSYDWLL2021024). The principles on ethical animal research outlined in the Basel Declaration and the ethical guidelines by the International Council for Laboratory Animal Science was followed.

Drugs and Reagents

The Sch D component herbs were provided by the Traditional Chinese Medicine Pharmacy at Wenzhou Traditional Chinese Medicine Hospital. The herbal medicines were formally identified by pharmacognosist Dr. Xuemei Zhu. The identification numbers for Schisandra, Ophiopogon, Panax, Cistanche, Cuscuta, Uncaria, Zingiber, and Ziziphus are (220503, 220,501, 220,506, 220,506, 220,422, 220,428, 220,401, 220,503). Schisandra, Ophiopogon, and Cistanche were obtained from Zhejiang Huayu Pharmaceutical Co., Ltd. (Drug Production License No. Zhe 20040348); Panax, Uncaria, Zingiber, and Ziziphus were sourced from Zhejiang University of Traditional Chinese Medicine Herbal Slice Co., Ltd. (Drug Production License No. Zhe 20000076); Cuscuta was provided by Zhejiang Tongjun Tang Traditional Chinese Medicine Herbal Slice Co., Ltd. (Drug Production License No. Zhe 20000072). The use of plant materials complies with local institutional regulations, and no additional approvals are required. Herbs were first soaked in double-steamed water for approximately 0.5 hours. Subsequently, the herbal materials were admixed with an 8-fold volume (v/w) of distillate and decocted for 60 minutes over gentle calefaction to eliminate the residual liquor. Next, the herbs were mixed with a 5-fold volume (v/w) of distilled water and boiled for another 60 minutes over low heat. The remaining liquids from the two boils were then collected, filtered and concentrated over low heat to a concentration of 2 g/mL. The concentrate was stored at 4°C until use.

MPTP (Shanghai Yuanye Biotechnology Co., Ltd., item number S31504-500mg); LY294002 (MedChemExpress, item number HY-10108); LC3 antibody, AKT antibody, p-AKT antibody, PTEN antibody, PI3K antibody, mTOR antibody, p-mTOR antibody, p70S6K antibody, p62/SQSTM1 antibody, α-syn antibody (Wuhan Biode Biotechnology Engineering Co., Ltd., item numbers: BM4827, BM1612, BM4762, A00006-1, PB0351, BM4182, BM4840, M01475-4, PB0458, M00215-3, respectively). TH antibody, Sodium citrate antigen repair solution, SignalStain® Boost Detection Reagent, SignalStain® DAB Substrate Kit (Cell Signaling Technology, item numbers: 58844S, 14746, 8125, 8059, respectively); dimethylbenzene, Neutral balsam (Sinopharm Chemical Reagent Co., Ltd., item numbers:10023418,10004160, respectively).

Equipment

A gauze-wrapped metal climbing rod (75 cm length, 9 mm diameter) was prepared as previously reported.[16] Open field testing was performed using a Kinder Scientific Company LLC model MM100CCSCCI apparatus. Rotary rod tests were performed using a UGO BASILE model 47650 apparatus. Real-Time Quantitative Polymerase Chain Reaction (RT-qPCR) was performed using an Illumina eco. Samples were centrifuged using a Thermo LEGEND MICRO 21R centrifuge. Protein preparations were electrophoresed using a Biorad model 1645050 apparatus.UPLC-Q-TOF/MS analysis was conducted using the Waters model SYNAPT G2-Si apparatus. Paraffin embedding was carried out using Thermo Shandon Histocentre 2. Paraffin sectioning was performed using Thermo Finesse 325. Observation and photography were conducted using Nexcope NE910 model.

Identification of Compounds in Sch D Using UPLC-Q-TOF/MS Technology

Identification of Compounds in Sch D using UPLC-Q-TOF/MS Technology: Liquid phase conditions consisted of 0.1% formic acid in water and pure acetonitrile. The large gradient method over 35 minutes was as follows: 0–2 minutes, 5% acetonitrile; 2–32 minutes, 5–100% acetonitrile; 32–33 minutes, 100% acetonitrile; 33.5 minutes, 5% acetonitrile; 33.5–35 minutes, 5% acetonitrile. The flow rate was set at 0.3 mL/min, injection volume at 2 μL, column temperature at 35°C, and sample chamber temperature at 10°C. Mass spectrometry method: ESI ion source, scanning in positive and negative ion modes, respectively. MSE continuous full scan mode with a scan time of 0.2 s and a scan range of 50~1200. Collision energy in MSE: low collision energy at 6 V, high collision energy ranging from 15 to 45 V. Sodium formate was utilized for mass spectrometer calibration, and leucine enkephalin (positive ion mode m/z 556.2771, negative ion mode m/z 554.2615) was employed for real-time mass calibration.

PD Mouse Model Preparation and Treatment Groups

Mice (N=50) were randomly assigned to either control (N=10) cohort or PD model (N=40) cohort. The PD model cohort was further randomly assorted into 4 treatment groups of 10 mice each: MPTP (treated with MPTP only), LY294002 (treated with MPTP plus the PI3K inhibitor LY294002), Sch D (treated with MPTP plus Sch D) and LY294002 + Sch D (treated with MPTP plus both LY294002 and Sch D) groups. After group assignation, MPTP only mice were injected intraperitoneally with 30 mg/kg MPTP diluted in saline (1 mg/mL) once daily over 7 consecutive days. Control cohort mice underwent a parallel saline injection regimen. Sch D group animals were simultaneously treated over the same time period with daily MPTP as described above and daily 0.75 g/100 g Sch D administered by gavage. LY294002 group animals were simultaneously treated over the same time period with daily MPTP as described above and once daily 50 mg/kg IP LY294002. LY294002 + Schisandra group mice were simultaneously treated over the same time period with daily MPTP plus LY294002 and Sch D as described above. During the 7 days model preparation and treatment period the mice were regularly monitored for changes in mental state, posture, appearance. A schematic illustration of the experimental design is shown in Figure 1.

Physical Performance and Behavior Testing

Forty-eight hours after the end of the model preparation and treatment period, mice were evaluated in pole climbing, rotary bar and open field tests as described below. All experiments were performed between 9 am and 12 noon. The testing apparatuses were thoroughly cleaned prior to the start of each test.

Pole climbing assay: Each mouse received 2 days of training on the climbing pole prior to testing. Testing was then completed in a single day. For testing, the animal was placed on the top of the climbing pole and the time required to turn around and climb from the top of the pole to the bottom was recorded. Both return time and total time were documented. For each animal the test was repeated 3 times, with a 30 min. interval between repetitions. The final climbing time for a given animal was determined as the average of the 3 measurements. If an animal reversed itself or ceased climbing, the test was repeated.

Rotary bar assay: Prior to testing, each mouse received 3 days of training on the rotary bar at a fixed speed of 10 rpm for 3 min. each day. For testing, an animal was placed on a static rotary bar for a period of 5 min. in order to acclimate. The rotary bar speed was then gradually increased to a max. velocity of 40 rpm. The time from initiation of walking until falling off from the rotary bar was recorded. For each animal the test was repeated 3 times, with a 30 min. interval between repetitions. The final walking time for a given animal was determined as the average of the 3 measurements.

Open field test: Mice were placed within the experimental field and observed for a period of 15 min. The duration and distance of locomotion circumscribing the perimeter and the center of the field were documented. Tests were conducted over a single day.

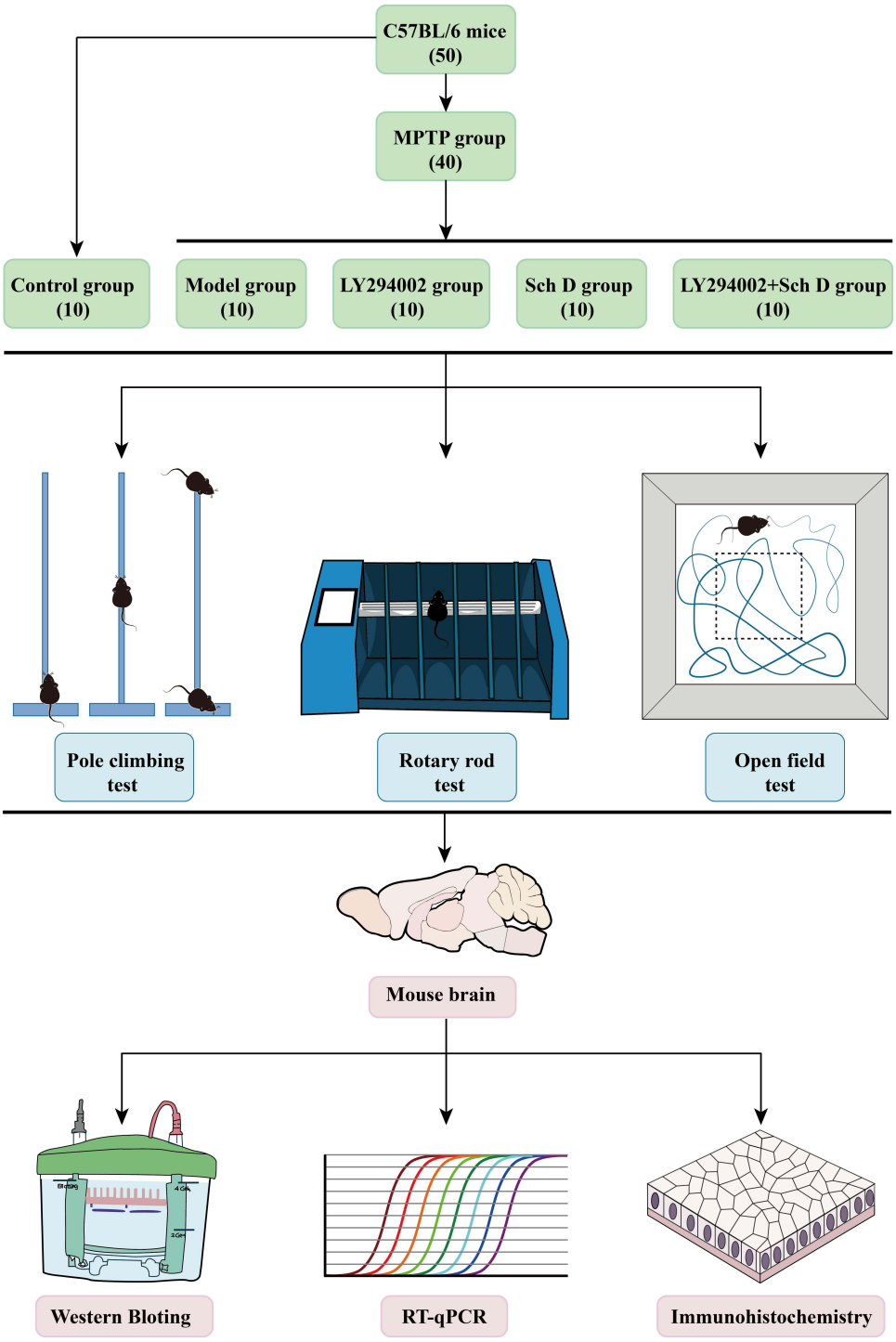

Figure 1 Schematic illustration of the experimental design.

Brain Tissue Preparation

Following physical performance and behavioral testing, mice were anaesthetized using 4% Isoflurane and then maintained anesthetized with 2%.Cervical dislocation method was used to euthanize the mice and collect brain tissues. The substantia nigra was rapidly separated from the brain coronal section on ice using a surgical blade, then fixed in 4% paraformaldehyde for 24 hours and dehydrated before freezing sectioning of brain tissues. The remaining portion was

frozen in liquid nitrogen for subsequent RT-qPCR analysis, while a portion was used for protein sample analysis with WB.

RT-qPCR Analysis

Total RNA was extracted from brain tissue using Trizol reagent. RNA concentration was determined by Nano drop2000 spectrophotometry (Thermo Fisher Scientific). cDNA was prepared using a HyperScript™ RT SuperMix for qPCR kit (APExBIO) according to the manufacturer's instructions. RT-qPCR was performed using a illumina eco PCR detection system β-actin as internal control, primer sequence was shown in Table 2.The relative expression levels of the target mRNAs were calculated as previously described.[17]

Western Blotting Analysis

Brain tissue was homogenized using a tissue grinder. The homogenate was rinsed twice with ice-cold phosphate buffered saline (PBS) and centrifuged at 12,000 rpm for 40 min. at 4 °C. The supernatant was collected, mixed with protein cracking solution and protease inhibitor, and incubated for 40 min. at 4 °C. Perform protein quantification according to the instructions of the BCA protein quantification kit (Beyotime Biotechnology). 20 μg of protein was electrophoresed (10% Sch DS gel) at 130 V for 90 min. and proteins were transferred to a PVDF membrane at 100 V for 1 hour. The membrane was blocked using 5% nonfat milk at 37 °C for 1 hour. Membrane strips were incubated with primary antibody overnight at 4°C, washed three times with PBS at room temperature, and incubated with ALP-labeled secondary antibody for 1 hour. After washing in PBS the protein levels were determined using a GelView 6000Plus (Guangzhou Boluoteng Biological Technology Co., Ltd). and image analysis software (Image J).

Immunohistochemistry

After embedding the mouse brain in Shandon Histocentre 2, slice it into 4μm thick sections using Finesse 32. Incubate the sections in Neutral balsam washing solution for 5 minutes × 3 times, then in 100% ethanol for 10 minutes × 2 times, and in 95% ethanol for 10 minutes × 2 times. Submerge the sections in 1× Sodium citrate antigen retrieval solution and maintain at boiling temperature for 10 minutes. After cooling, wash with dH2O for 5 minutes × 3 times. Incubate in 3% hydrogen peroxide solution for 10 minutes, then wash with dH2O for 5 minutes × 2 times, followed by a 5-minute wash in 1× PBS. Block the sections with 200 μL blocking solution at room temperature for 1 hour, then incubate overnight at 4°C with the primary antibody diluted 1:500. Bring the SignalStain® Boost Detection Reagent to room temperature, wash with 1× PBS for 5 minutes × 3 times, and apply 200 μL of SignalStain® DAB for staining. Wash with dH2O, dehydrate the sections, incubate in Neutral balsam, and cover-slip for photography.

Statistical Analysis

All data were analyzed using GraphPad Prism 9.4.1 software. To ensure the validity of the data analysis, we first conducted tests for normality and homogeneity of variances. Normality was assessed using the Shapiro–Wilk test to confirm whether the data followed a normal distribution. Homogeneity of variances was evaluated using the Brown-

Table 2 Primer Sequence

Gene Name	Bidirectional Primer Sequence
PI3K	F 5′- TGTGCAGCCAAGGAACCG-3′
	R 5′-TCTCAGCTTCACCTCCGGGT-3′
PTEN	F 5′-AGGACCAGAGACAAAAAGGGAG-3′
	R 5′-CGGGTCTGTAATCCAGGTGAT-3′
LC3	F 5′-AAGAGTGGAAGATGTCCGGC-3′
	R 5′-TCGCTCTATAATCACCCGCC-3′
GAPDH	F 5′-TGGAAGGGCTCATGACCACAG-3′
	R 5′-GGGGTCTGGGATGGAAATTGT-3′

Forsythe test to assess whether the variances across groups were equal. Given that the assumptions of normality and homogeneity of variances were met, we performed a one-way Analysis of Variance (ANOVA) to detect overall differences in means among the groups. ANOVA was used to test whether there were significant differences between group means. Subsequently, Tukey's Honestly Significant Difference Test (HSD) was employed for post-hoc multiple comparisons to determine which specific group pairs had significant differences. A significance level of $P < 0.05$ was considered statistically significant.

Results

Identification of Compounds in Sch D

The test medicinal material solution was analyzed under the specified chromatography and mass spectrometry conditions. Combining the obtained results with literature references, the total ion chromatogram and components in positive and negative ion modes are presented in Figure 2.

Effects of Treatments on Physical Performance and Behavior

Consistent with previous reports,[7] PD model mice (treated with MPTP only) took longer (in terms of both return and total times) to complete the test compared to control mice (Figure 3A and B). Test times were further lengthened for MPTP model mice treated with the PI3K inhibitor LY294002. Treatment with Sch D significantly reduced test times (Figure 3A and B), though this effect was attenuated for mice treated with both Sch D and LY294002.

As shown in Figure 3C, MPTP induced PD model mice displayed a significant reduction in the duration of time spent on the rotary rod compared to control mice. The latency period was further reduced by treatment with LY294002. Administration of Sch D significantly extended the time spent on the rotary rod compared to model group mice and attenuated the reduced latency effect of LY294002 (Figure 3C).

MPTP induced PD model mice exhibited reduced exploratory travel distance both at the periphery and in the center of the open field compared to control mice (Figure 3D–F). The center distance/periphery distance ratio was also reduced for model mice relative to controls. The same effect, though to different magnitudes, was observed among mice treated with LY294002. Sch D treatment partially attenuated the effects observed among model mice with respect to distance traveled at periphery and center, and there was no significant difference between control and Schisandra group mice in terms of the center distance/periphery distance ratio (Figure 3D–F). The degree of Schisandra treatment-associated attenuation of exploratory travel defects was lower among mice co-treated with LY294002. Figure (Figure 3G–I) shows that control

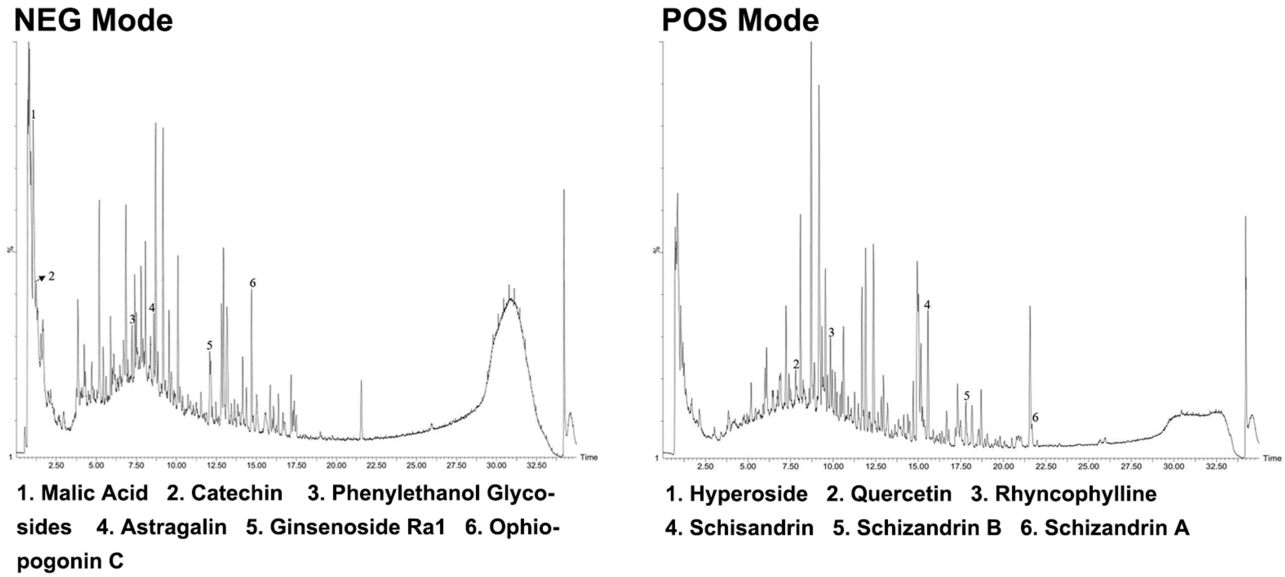

Figure 2 UPLC-Q-TOF/MS Total Ion Chromatogram of Sch D.

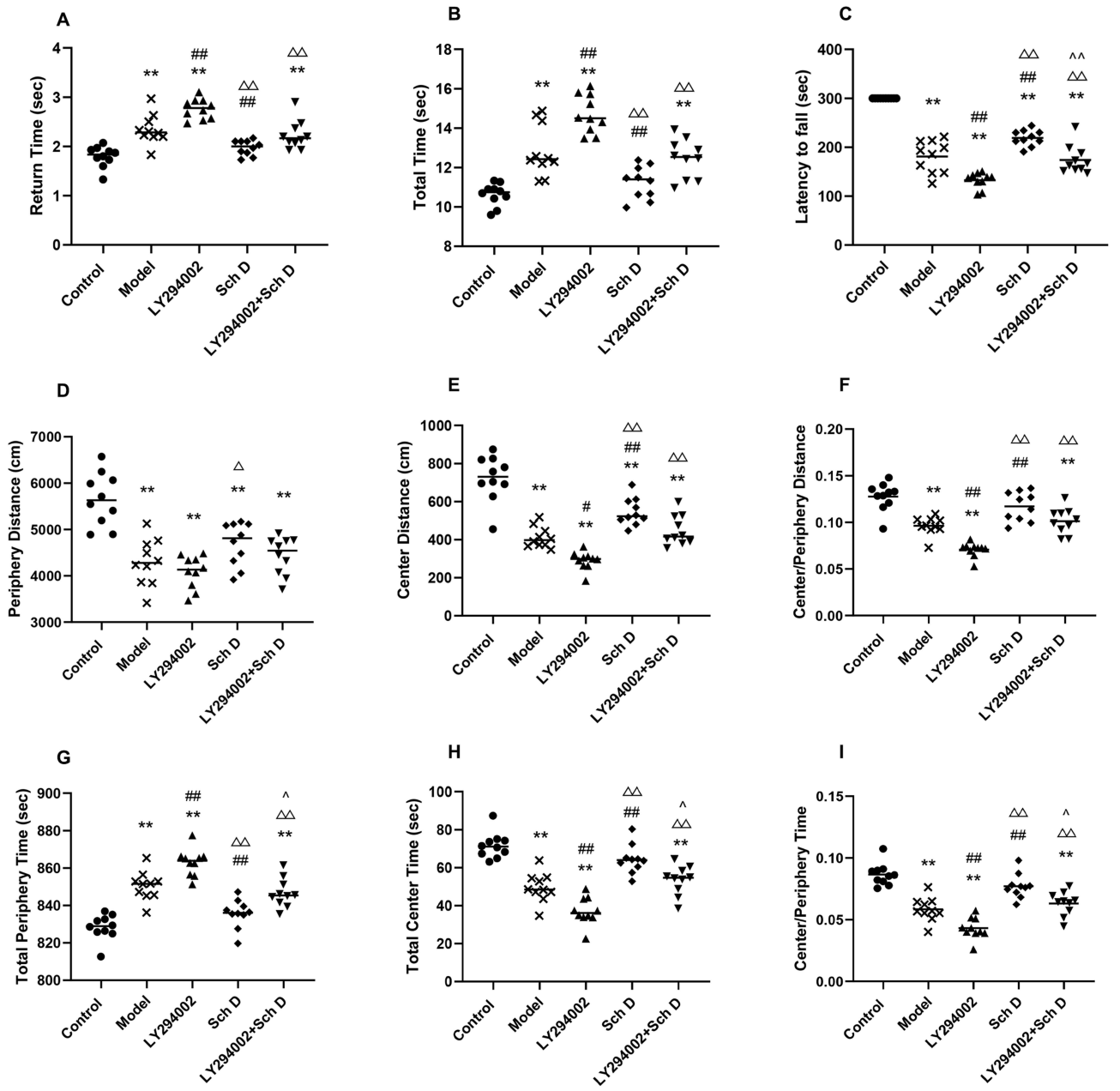

Figure 3 Behavioral results. (**A**) Pole climbing assay return time. (**B**) Pole climbing assay total time. (**C**) Rotary assay results. (**D**) Open field test peripheral distance traveled. (**E**) Open field test central distance traveled. (**F**) Open field test ratio of central distance/ peripheral distance traveled. (**G**) Open field test total time at periphery. (**H**) Open field test total time in center. (**I**) Open field test time in center/periphery. Use the Tukey HSD test statistical method. ** P < 0.01 compared to control group; # P < 0.05 compared to model group. ## P < 0.01 compared to model group. (ie MPTP only) group; Δ P < 0.05 compared to LY294002 group. ΔΔP < 0.01 compared to LY294002 group. ^ P < 0.05 compared to Sch D group. ^^ P < 0.01 compared to Sch D group.

mice spent significantly less total time at the periphery and more total time in the center of the open field than model mice and LY294002 treated mice. Significant differences were also observed between control mice and both model mice and LY294002 treated mice in terms of central retention time/peripheral retention time ratios. By contrast, mice treated with Schisandra did not differ significantly from control mice in terms of total time at periphery or center. Furthermore, Schisandra attenuated the adverse effects of LY294002 (Figure 3G–I).

Effect of Sch D on α-Syn, TH and Autophagy-Related Protein Expression Abundance

Model and treatment group mice all exhibited significantly elevated levels of α-syn compared to controls (Figure 4A and B). Sch D treatment was associated with significantly less α-syn compared to LY294002 treated mice.

In comparison to the control group, both the Model group and the LY294002 group showed a decrease in TH levels, with the LY294002 group exhibiting a more significant reduction ($P < 0.01$). This situation was reversed after the use of Sch D, with the reversal being even more pronounced in the Parkinson's model mice treated solely with Sch D ($P < 0.01$) (Figure 4C–E).

WB analysis revealed significantly upregulated LC3II/I protein expression in model, LY294002 and LY294002 + Sch D group mice relative to control group mice ($P < 0.01$). Sch D treatment was associated with reduced abundance of LC3II/I relative to LY294002 group mice ($P < 0.01$) (Figure 5A and B). Abundance of p62 was decreased in model and LY294002 group mice relative to controls ($P < 0.05$ and $P < 0.01$, respectively). Sch D treatment, alone or in combination with LY294002, was associated with significantly increased abundance of p62 compared to LY294002 group mice (Figure 5A and C). As shown by RT-qPCR analysis Figure 5D, levels of LC3 mRNA were increased in model and experimental treatment groups relative to controls ($P < 0.01$). LY294002 group mice had higher levels of LC3 mRNA than model mice ($P < 0.01$). LC3 mRNA levels were significantly reduced relative to LY294002 group mice in the Sch D and LY294002 + Sch D treated animals ($P < 0.01$).

Effect of Sch D on PI3K/AKT/mTOR Signaling Pathway

WB analysis (Figure 6A–C) showed significantly increased levels of PTEN and significantly decreased levels of PI3K proteins in model, LY294002 and LY294002 + Schisandra groups compared to controls. LY294002 treated mice exhibited marked differences in protein abundance compared to model animals. Sch D treated mice also tended toward

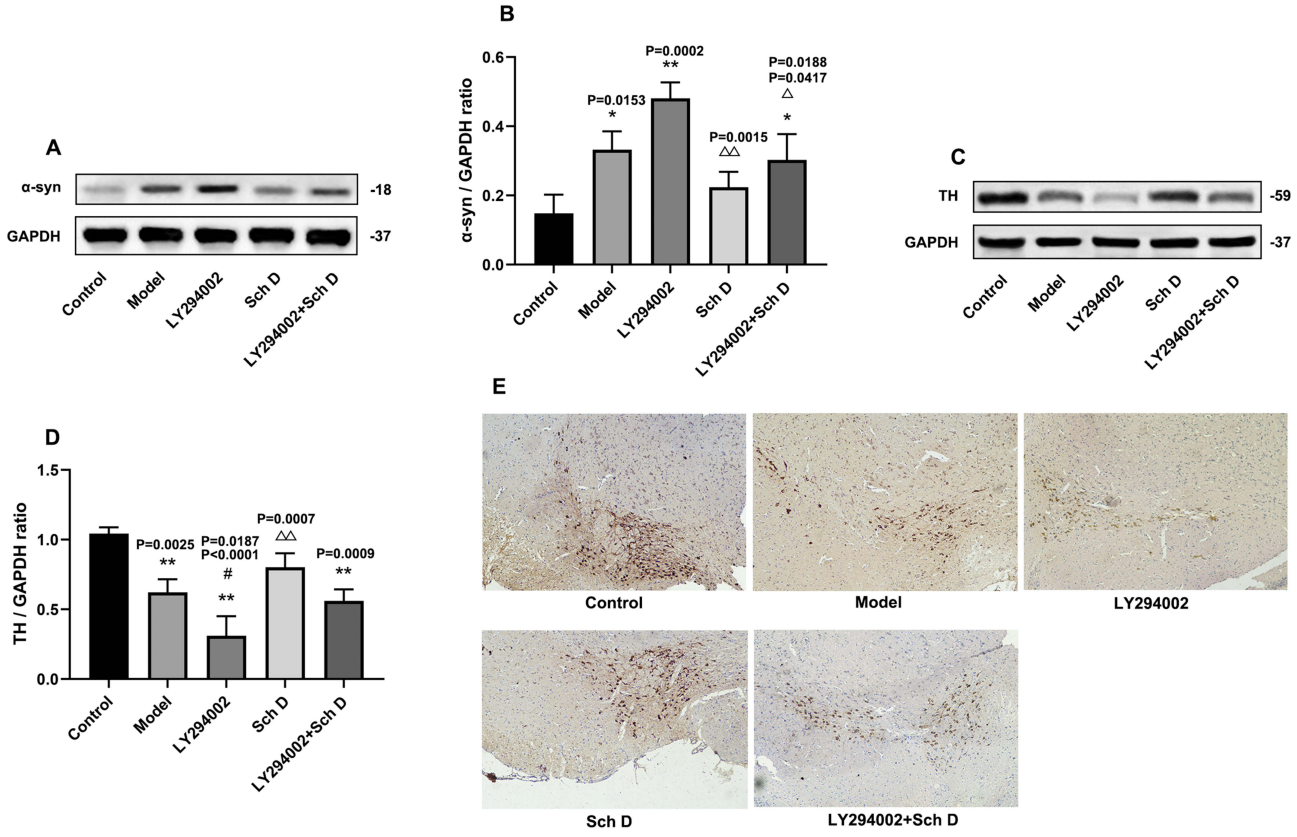

Figure 4 α-Syn protein levels. (**A**) WB electrophoretogram of α-syn and GAPDH. (**B**) Relative abundance of α-syn across treatment groups. (**C**) WB electrophoretogram of TH and GAPDH. (**D**) Relative abundance of TH across treatment groups. (**E**) TH immunohistochemistry diagram. Use the Tukey HSD test statistical method. * P < 0.05, ** P < 0.01 compared to control group. # P < 0.05 compared to model group. ΔP < 0.05, ΔΔ P < 0.01 compared to LY294002 treatment group.

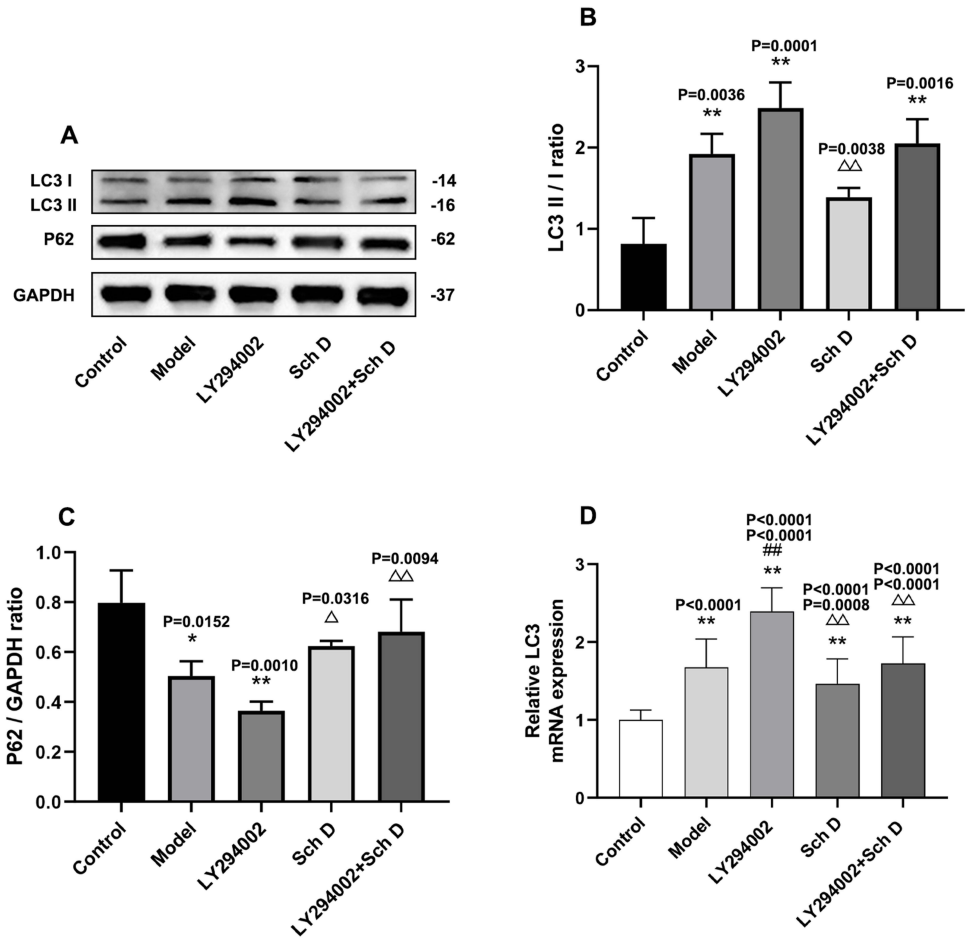

Figure 5 Relative abundance of autophagy-related proteins LC3 and p62/SQSTM and LC3 mRNA. (**A**) LC3 I, LC3II and p62 WB electrophoretogram. (**B**) Relative level of LC3 II / I protein. (**C**) Relative level of p62 protein. (**D**) Relative level of LC3 mRNA. Use the Tukey HSD test statistical method. * P < 0.05, ** P < 0.01 compared to controls. ## P < 0.01 compared to model group. Δ P < 0.05, ΔΔ P < 0.01 compared to LY294002 group.

increased PTEN and decreased PI3K relative to control animals, but this treatment group showed lesser degrees of abnormality. Co-administration of Sch D with LY294002 was found to mitigate the effect of LY294002 on PTEN but not PI3K abundance. RT- qPCR analysis showed that relative abundances of PTEN and PI3K mRNAs essentially mirrored the results of protein analysis (compare Figure 6D and E to B and C).

WB analysis showed reduced phosphorylation of AKT and mTOR and lower levels of p70S6K proteins in model mice and all treatment groups relative to controls (Figure 7). LY294002 treatment was associated with significantly lower levels of AKT and mTOR phosphorylation and p70S6K abundance than model mice. Compared to LY294002 mice, animals treated with Sch D (alone and in combination with LY294002) exhibited higher levels of AKT and mTOR phosphorylation and increased abundance of p70S6K.

Discussion

PD is an incurable neurodegenerative disorder characterized by numerous severe complications. Over time, patients lose the ability to care for themselves, eventually succumbing to issues such as hyponatremia and heart failure.[18–20] The primary pathological features of PD include the degeneration of dopaminergic neurons in the substantia nigra (SN), reduced DA levels in the striatum, and the accumulation of misfolded α-syn.[21] Current PD treatments, including dopamine replacement therapy, mainly address symptoms but fail to slow disease progression,[22] underscoring the urgent need for novel therapeutic strategies. In this study, we employed an MPTP-induced PD mouse model to investigate the effects of Sch D, a traditional Chinese medicine, on motor performance and behavior. Our goal was to evaluate the

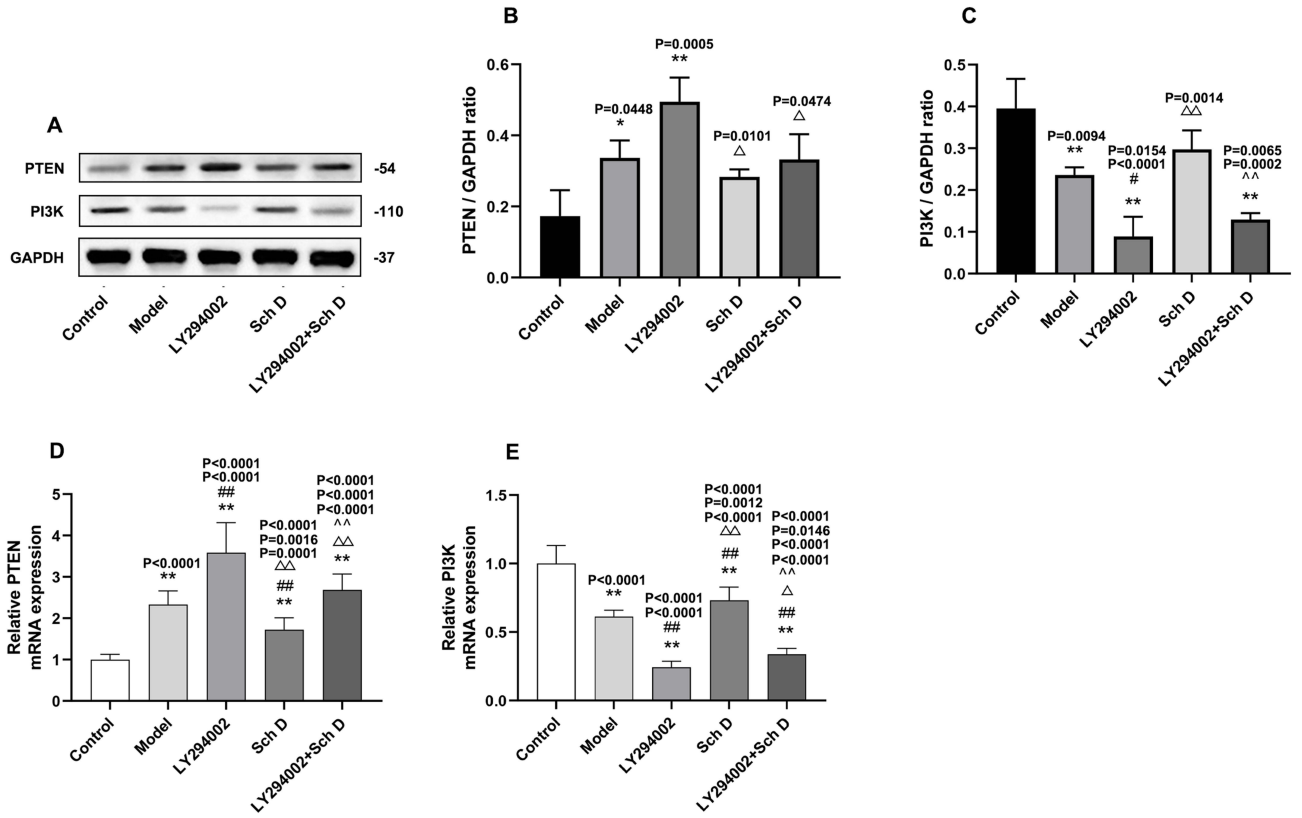

Figure 6 Relative abundance of PTEN and PI3K proteins and transcripts. (**A**) WB electrophoretogram. (**B**) and (**C**). Relative abundance of PTEN and PI3K proteins, respectively. (**D**) and (**E**) Relative abundance of PTEN and PI3K mRNAs, respectively. Use the Tukey HSD test statistical method. * P < 0.05, ** P < 0.01 compared to control. # P < 0.05, ## P < 0.01 compared to model group. △ P < 0.05, △△P < 0.01 compared to LY294002 group. ^^ P < 0.01 compared to Sch D group.

neuroprotective effects of Sch D in PD model mice and explore its potential as a new clinical treatment for the disease. The neuroprotective mechanism of Sch D on PD mice is shown in Figure 8. The MPTP-induced model is widely recognized as one of the most reliable models for studying PD. Previous studies have shown that systemic administration of MPTP in both non-human primates and mice causes irreversible, selective degeneration of substantia nigra dopaminergic neurons, mimicking the disease's progression in humans. MPTP, a highly lipophilic molecule, crosses the blood-brain barrier and is metabolized by astrocytic monoamine oxidase B into 1-methyl-4-phenylpyridinium (MPP+), a hydrophilic metabolite. MPP+ disrupts ATP production, elevates intracellular calcium levels, and increases the production of reactive oxygen species (ROS) and reactive nitrogen species, leading to dopaminergic neuron apoptosis. By selectively targeting these neurons, MPTP induces symptoms that closely resemble those of human PD.[23,24] TH, a highly specific rate-limiting enzyme in dopamine synthesis, plays a critical role in maintaining dopaminergic neuron function. A reduction in TH expression in the substantia nigra is closely associated with the loss of dopaminergic neurons, accelerating PD progression.[25] Our findings demonstrate that Sch D treatment significantly increases TH expression and reduces α-syn levels in the substantia nigra of MPTP-induced PD model mice. This aligns with previous studies, suggesting that Sch D provides significant neuroprotection against DA neuron loss in this model.[26] In behavioral assessments, mice treated with Sch D exhibited superior performance in the pole test, rotarod test, and open field test, indicating improvements in motor function. These results highlight the potential of Sch D to ameliorate motor deficits in PD and offer a promising avenue for future clinical treatments.

LY294002 is a synthetic morpholine derivative commonly used as a PI3K inhibitor, capable of inhibiting the PI3K/AKT pathway by suppressing AKT phosphorylation.[27] This study shows that following the inhibition of PI3K/AKT pathway activation by LY294002, the levels of p-PI3K/PI3K, p-Akt/Akt, and p-mTOR/mTOR proteins were downregulated, while the protein level of PTEN, a negative regulator of PI3K, was upregulated, and p70s6k, a direct substrate of mTOR, was downregulated. Conversely, Sch D exhibited an opposite effect on this pathway. Sch D increased the

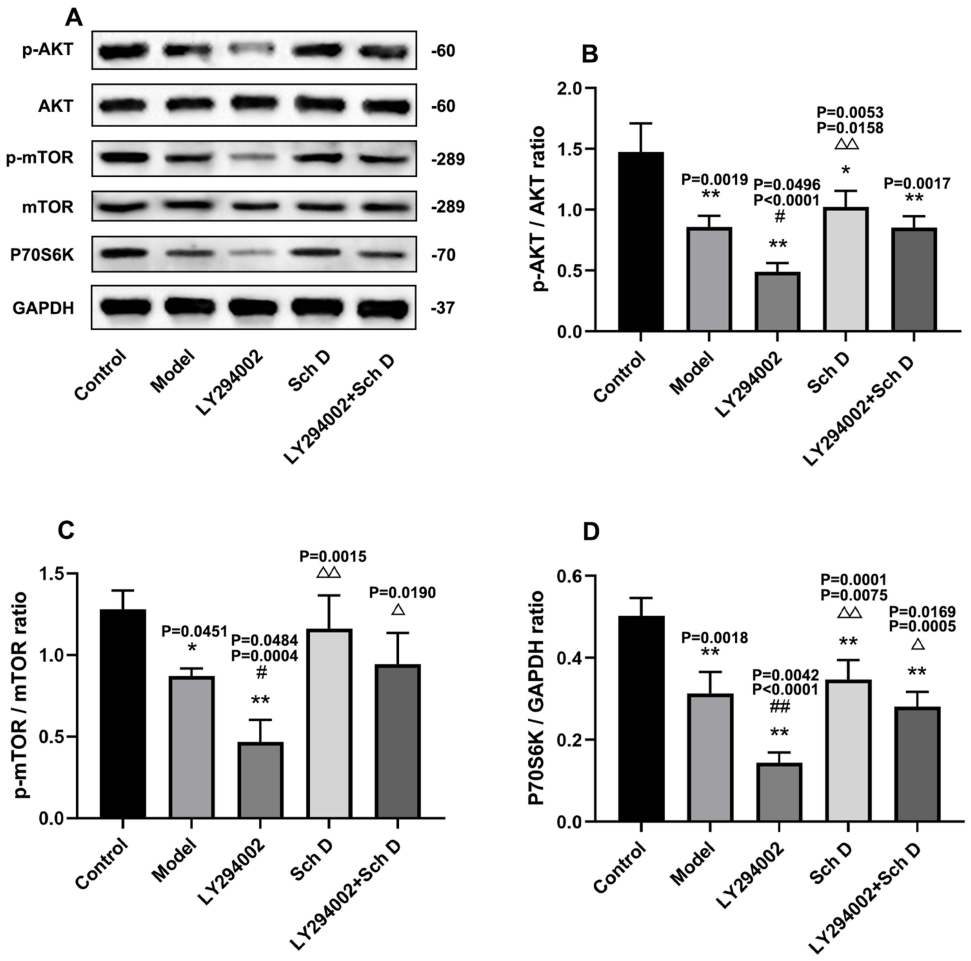

Figure 7 AKT and mTOR phosphorylation and relative abundance of p70S6K. (**A**) WB electrophoretogram. (**B**) and (**C**) Relative degree of AKT and mTOR phosphorylation. (**D**) Relative abundance of p70S6K. Use the Tukey HSD test statistical method. *P < 0.05, **P < 0.01 compared to control. # P < 0.05, ## P < 0.01 compared to model group. Δ P < 0.05, ΔΔ P < 0.01 compared to LY294002 group.

phosphorylation levels of PI3K, Akt, and mTOR in the brains of PD model mice. This may be due to the downregulation of PTEN protein induced by Sch D, which reduced the inhibition of PI3K signaling and activated the PI3K/AKT/mTOR pathway, subsequently upregulating p70s6k, a direct substrate of mTOR. The PI3K/AKT/mTOR signaling pathway is a key regulatory pathway of autophagy under specific conditions, and disruption or deregulation of the autophagy system is closely related to neurodegenerative diseases.[28,29] Akt, also known as PKB, is a downstream effector of PI3K and acts as a major positive regulator of mTOR activity.[30,31] The activation of AKT is influenced by various regulatory mechanisms, and it can be phosphorylated at two sites, Thr308 and Ser473.[32] Activated PI3K generates PIP3, which recruits PDK1 and AKT to the cell membrane, allowing PDK1 to phosphorylate AKT at Thr308, thereby activating AKT.[33] Akt plays a crucial role in the development of PD, and research has shown that the activation of Akt can reduce damage to midbrain dopaminergic neurons.[34] This aligns with our findings that Sch D upregulates Akt levels, reduces α-syn aggregation in the brains of mice, and increases TH protein expression. PTEN is an important negative regulator of the PI3K/AKT signaling pathway. It has the enzymatic activity to dephosphorylate PIP3, converting it into PIP2, thus limiting the activation of the signaling pathway.[35] Loss or malfunction of PTEN can lead to excessive activation of the PI3K/AKT pathway.

The changes in the PI3K/Akt/mTOR pathway are closely related to the activation of autophagy. Targeting PI3K/AKT/mTOR-mediated autophagy is a key therapeutic strategy for various tumors.[36] Moreover, several studies have found that this pathway is also involved in the regulation of autophagy in the treatment of osteoarthritis, polycystic ovary syndrome, and neurodegenerative diseases.[37–39] Markers of autophagy activity include the ratio of autophagy-related proteins LC3II

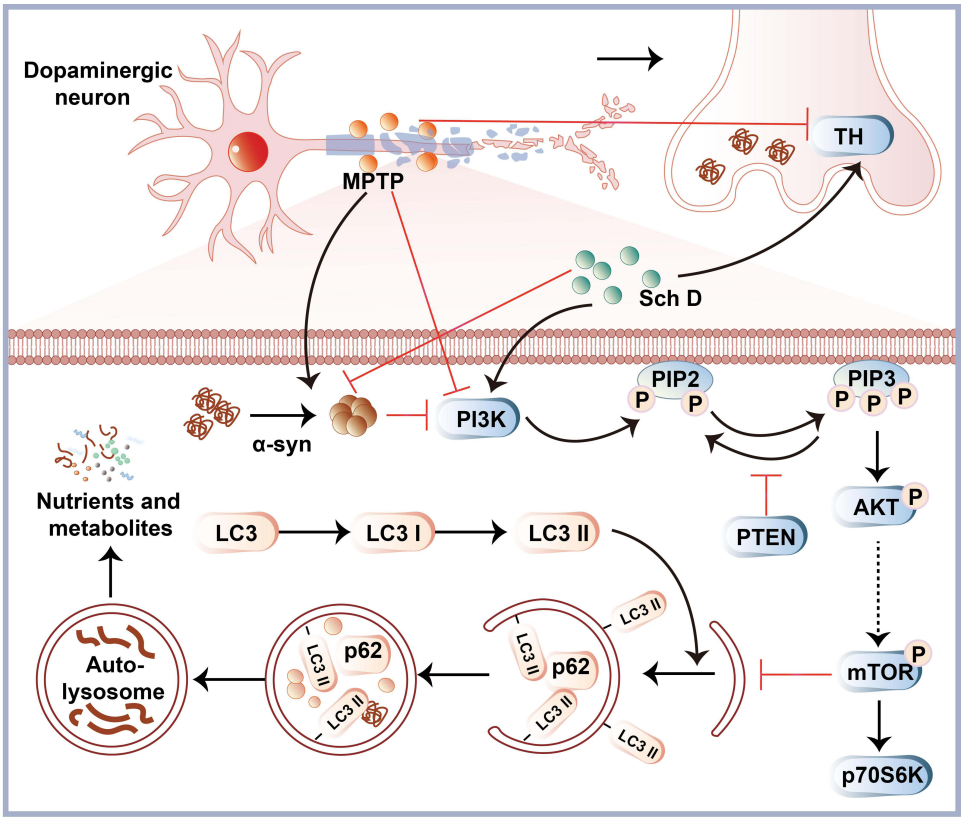

Figure 8 Mechanism of action of Sch D on Parkinson's mice.

to LC3I and the level of the autophagosome membrane scaffold protein p62. p62, a well-studied autophagy substrate, acts as a bridge between LC3 and polyubiquitinated proteins during autophagosome formation, being selectively incorporated into autophagosomes and subsequently degraded by autolysosomal proteases. Therefore, p62 protein expression is negatively correlated with autophagy activity.[40] Under normal physiological conditions, autophagy is maintained at relatively low levels. Once cellular damage occurs, such as oxidative stress, protein aggregation, or organelle damage, autophagy activity rapidly increases.[41] Previous studies have shown that excessive production of reactive oxygen species (ROS), oxidative stress, and mitochondrial dysfunction contribute to the onset of PD.[42,43] Moreover, neurotoxins that induce degeneration of dopaminergic neurons, including MPTP, can induce ROS formation, which leads to enhanced autophagy. Studies have found that the PI3K α catalytic subunit inhibits autophagy, while its β catalytic subunit responds to changes in ROS levels to promote autophagy.[44] The MPTP-induced PD mouse model may activate autophagy by inhibiting PI3K protein levels through the induction of ROS. Numerous studies have shown that many natural compounds exhibit neuroprotective effects in MPTP-induced PD models due to their antioxidant properties. For example, pterostilbene exerts neuroprotective effects in PD mice by reducing ROS and malondialdehyde levels and increasing total antioxidant capacity and superoxide dismutase activity.[45] Similarly, Withania somnifera protects striatal dopaminergic neurons by reducing oxidative stress markers such as iNOS expression and pro-inflammatory markers.[46] The bioactive component ursolic acid of Withania somnifera has been shown to protect dopaminergic neurons.[47] Additionally, Mucuna pruriens reduces iNOS expression and alleviates MPTP neurotoxicity.[48,49] Similar to previous studies, many components of Sch D in this study also exhibit antioxidant effects. For example, α-Iso-cubebene, one of the main constituents of Schisandra chinensis, exerts anti-vascular inflammatory effects by inhibiting ROS production, thereby suppressing HMGB1-induced monocyte-to-macrophage differentiation.[50] Additionally, alkaloids extracted from Uncaria have been shown to exert anti-PD effects by reducing ROS production.[51] Other herbal components in Sch D, such as ginsenosides, Cistanche deserticola polysaccharides, and Cuscuta chinensis flavonoids, also possess antioxidant properties.[52–54] In this study, we observed that, compared with control mice, MPTP-induced PD model mice exhibited increased LC3 mRNA

expression, a higher LC3II/I ratio, and reduced p62 levels, which are consistent with enhanced autophagy. At the same time, MPTP mice also had lower TH protein levels and more α-syn accumulation. These results suggest that MPTP-induced oxidative stress may trigger excessive autophagy by activating the PI3K/Akt/mTOR signaling pathway, leading to neuronal death and promoting PD pathology and symptoms. This finding aligns with previous studies that suggest excessive neurotoxicity and misfolded protein aggregates lead to neuronal death through the activation of autophagy and apoptotic pathways.[55] We also observed abnormal activation of autophagy markers in LY294002-treated PD model mice, which may be related to the specific inhibition of PI3K by this compound. In contrast, Sch D-treated mice exhibited a lower LC3II/I ratio, lower LC3 mRNA expression, and higher p62 levels, indicating reduced autophagy activity. Similar to our findings, a study on autophagy-related non-coding RNAs reported that increases in BDNF-AS and SNHG1 reduced autophagy in MPTP-induced PD by targeting miR-125b-5p and miR-221/222, respectively.[56] However, Sch D-treated mice showed higher TH protein levels and lower α-syn levels. This finding, which contrasts with the commonly held view that promoting autophagy reduces α-syn, may be explained by the complex composition of Sch D, which contains multiple antioxidant components. In future studies, we could assess the impact of Sch D on oxidative stress markers (eg, ROS, aquaporins, glutathione) to evaluate its antioxidant effects. By comparing the correlation between α-syn aggregation and oxidative stress levels, we can verify whether Sch D reduces α-syn accumulation by indirectly reducing oxidative stress. Additionally, although autophagy plays a positive role in clearing α-syn, excessive or inappropriate autophagy may also lead to cell death and pathological changes. Sch D may protect neurons and reduce pathological damage by moderately inhibiting autophagy to prevent excessive autophagy. Moreover, the timing of Sch D treatment may influence its effect on autophagy. Early Sch D treatment may activate autophagy to reduce α-syn, while long-term Sch D use could reduce α-syn through a feedback mechanism that activates the PI3K/AKT/mTOR pathway to inhibit autophagy. Future studies could observe PD mouse models treated with Sch D at different time points (eg, short-term, mid-term, long-term) to track changes in autophagy-related markers over time, allowing for dynamic observation of Sch D's regulatory effects on autophagy at various stages. Furthermore, Sch D may degrade α-syn through other pathways (such as the ubiquitin-proteasome pathway).[57] By measuring the levels of ubiquitinated proteins and proteasome activity, we can further verify the mechanism by which Sch D clears α-syn.

Through these future studies, we can gain a deeper understanding of the neuroprotective effects of Sch D via different mechanisms and further explore its potential for treating PD.

Conclusion

In summary, we show that Sch D improved TH, alleviated MPTP-induced PD symptoms and pathology-linked overexpression of α-syn in the brains of PD model mice. Schisandra treatment was associated with activation of the PI3K/Akt/mTOR signaling pathway, which we suggest may exert neuroprotective effects through the downregulation of excessive autophagy.

Abbreviations

ANOVA, one-way Analysis of Variance; AMPK, Adenosine 5′-monophosphate-activated protein kinase; α-syn, α-synuclein; DA, dopamine; GSH, glutathione; HSD, Tukey's Honestly Significant Difference Test; MPP+, 1-methyl-4-phenylpyridinium; MPTP, 1-methyl-4-phenyl-1,2,3,6-tetrahydropyridine; mTOR, mammalian target of rapamycin; PD, Parkinson's disease; PKB, protein kinase; ROS, reactive oxygen species RT-qPCR, Quantitative real-time PCR; Sch D, Schisandra Decoction; SN, substantia nigra; ULK, Unc-51-like kinases; WB, Western blotting.

Data Sharing Statement

Data are available on reasonable request. All supporting data within the article will be made available by the corresponding author.

Author Contributions

All authors made significant contributions to the work reported, including conception, study design, execution, acquisition of data, analysis, and interpretation; took part in drafting, revising, or critically reviewing the article; gave final

approval of the version to be published; agreed on the journal to which the article was submitted; and agree to be accountable for all aspects of the work.

Funding

This study was funded through the Basic Public Welfare Research Program of Zhejiang Province (Project number: LGF22H250004). Cultivation of National Excellent Clinical Talents of Traditional Chinese Medicine (National Traditional Chinese Medicine Ren Jiao Han [2022] No. 1).

Disclosure

The authors report no conflicts of interest in this work.

References

1. Armstrong MJ, Okun MS. Diagnosis and Treatment of Parkinson Disease: a Review. *JAMA*. 2020;323(6):548–560. doi:10.1001/jama.2019.22360
2. Li W, Jiang Y, Wang Y, et al. MiR-181b regulates autophagy in a model of Parkinson's disease by targeting the PTEN/Akt/mTOR signaling pathway. *Neurosci Lett*. 2018;675:83–88. doi:10.1016/j.neulet.2018.03.041
3. H-Y T, Yuan B-S, Hou X-O, et al. alpha-synuclein suppresses microglial autophagy and promotes neurodegeneration in a mouse model of Parkinson's disease. *Aging Cell*. 2021;20(12):e13522. doi:10.1111/acel.13522
4. Chartier-Harlin M-C, Jennifer K, Roumier C, et al. Alpha-synuclein locus duplication as a cause of familial Parkinson's disease. *Lancet*. 2004;364 (9440):1167–1169. doi:10.1016/S0140-6736(04)17103-1
5. Winslow AR, Chen C-W, Corrochano S, et al. α-Synuclein impairs macroautophagy: implications for Parkinson's disease. *J Cell Biol*. 2010;190 (6):1023–1037. doi:10.1083/jcb.201003122
6. Cicchini M, Karantza V, Xia B. Molecular pathways: autophagy in cancer--A matter of timing and context. *Clin Cancer Res*. 2015;21(3):498–504. doi:10.1158/1078-0432.CCR-13-2438
7. Menzies FM, Fleming A, Rubinsztein DC. Compromised autophagy and neurodegenerative diseases. *Nat Rev Neurosci*. 2015;16(6):345–357. doi:10.1038/nrn3961
8. Hasegawa J, Maejima I, Iwamoto R, Yoshimori T. Selective autophagy: lysophagy. *Methods*. 2015;75:128–132. doi:10.1016/j.ymeth.2014.12.014
9. Polchi A, Magini A, Meo DD, Tancini B, Emiliani C. mTOR Signaling and Neural Stem Cells: the Tuberous Sclerosis Complex Model. *Int J Mol Sci*. 2018;19(5):1474. doi:10.3390/ijms19051474
10. Saxton R, Sabatini D. mTOR Signaling in Growth, Metabolism, and Disease. *Cell*. 2017;168(6):960–976. doi:10.1016/j.cell.2017.02.004
11. Han L, Xie Y-H, Wu R, Chen C, Zhang Y, Wang X-P. Traditional Chinese medicine for modern treatment of Parkinson's disease. *Chin J Integr Med*. 2017;23(8):635–640. doi:10.1007/s11655-016-2537-7
12. Zhang Y, Wang -Z-Z, Sun HM, Ping L, Li Y-F, Chen N-H. Systematic review of traditional Chinese medicine for depression in Parkinson's disease. *Am J Chin Med*. 2014;42(5):1035–1051. doi:10.1142/S0192415X14500657
13. Han Y, Wang T, Li C, et al. Ginsenoside Rg3 exerts a neuroprotective effect in rotenone-induced Parkinson's disease mice via its anti-oxidative properties. *Eur J Pharmacol*. 2021;909:174413. doi:10.1016/j.ejphar.2021.174413
14. Li X, Zhang J, Zhang X, Dong M. Puerarin suppresses MPP/MPTP-induced oxidative stress through an Nrf2-dependent mechanism. *Food Chem Toxicol*. 2020;144:111644. doi:10.1016/j.fct.2020.111644
15. Zhi Y, Jin Y, Pan L, Zhang A, Liu F. Schisandrin A ameliorates MPTP-induced Parkinson's disease in a mouse model via regulation of brain autophagy. *Arch. Pharmacal Res*. 2019;42(11):1012–1020. doi:10.1007/s12272-019-01186-1
16. Kam T-I, Park H, Chou S-C, et al. Amelioration of pathologic alpha-synuclein-induced Parkinson's disease by irisin. *Proc Natl Acad Sci USA*. 2022;119(36):e2204835119. doi:10.1073/pnas.2204835119
17. Qian C, Ye Y, Mao H, et al. Downregulated lncRNA-SNHG1 enhances autophagy and prevents cell death through the miR-221/222 /p27/mTOR pathway in Parkinson's disease. *Exp Cell Res*. 2019;384(1):111614. doi:10.1016/j.yexcr.2019.111614
18. Adrogué HJ, Tucker BM, Madias NE. Diagnosis and Management of Hyponatremia: a Review. *JAMA*. 2022;328(3):280–291. doi:10.1001/jama.2022.11176
19. Gonçalves VC, Cuenca-Bermejo L, Fernandez-Villalba E, et al. Heart Matters: cardiac Dysfunction and Other Autonomic Changes in Parkinson's Disease. *Neuroscientist*. 2022;28(6):530–542. doi:10.1177/1073858421990000
20. Schapira AHV, Chaudhuri KR, Jenner P. Non-motor features of Parkinson disease. *Nat Rev Neurosci*. 2017;18(7):435–450. doi:10.1038/nrn.2017.62
21. Pajares M, IR A, Manda G, Boscá L, Cuadrado A. Inflammation in Parkinson's Disease: mechanisms and Therapeutic Implications. *Cells*. 2020;9 (7):1687. doi:10.3390/cells9071687
22. Wang R, Shih LC. Parkinson's disease - current treatment. *Curr Opin Neurol*. 2023;36(4):302–308. doi:10.1097/WCO.0000000000001166
23. Narmashiri A, Abbaszadeh M, Ghazizadeh A. The effects of 1-methyl-4-phenyl-1,2,3,6-tetrahydropyridine (MPTP) on the cognitive and motor functions in rodents: a systematic review and meta-analysis. *Neurosci Biobehav Rev*. 2022;140:104792. doi:10.1016/j.neubiorev.2022.104792
24. Obata T. Nitric oxide and MPP+-induced hydroxyl radical generation. *J Neural Transm*. 2006;113(9):1131–1144. doi:10.1007/s00702-005-0415-0
25. Zhou ZD, Saw WT, PGH H, et al. The role of tyrosine hydroxylase-dopamine pathway in Parkinson's disease pathogenesis. *Cell Mol Life Sci*. 2022;79(12):599. doi:10.1007/s00018-022-04574-x
26. Su CF, Jiang L, Zhang XW, Iyaswamy A, Li M. Resveratrol in Rodent Models of Parkinson's Disease: a Systematic Review of Experimental Studies. *Front Pharmacol*. 2021;12:644219. doi:10.3389/fphar.2021.644219
27. Feldman ME, Shokat KM. New inhibitors of the PI3K-Akt-mTOR pathway: insights into mTOR signaling from a new generation of Tor Kinase Domain Inhibitors (TORKinibs). *Curr Top Microbiol Immunol*. 2010;347:241–262. doi:10.1007/82_2010_64

28. Zhang Z, Yang X, Song YQ, Tu J. Autophagy in Alzheimer's disease pathogenesis: therapeutic potential and future perspectives. *Ageing Res Rev*. 2021;72:101464. doi:10.1016/j.arr.2021.101464
29. Youn JK, Kim DW, Kim ST, et al. PEP-1-HO-1 prevents MPTP-induced degeneration of dopaminergic neurons in a Parkinson's disease mouse model. *BMB Rep*. 2014;47(10):569–574. doi:10.5483/BMBRep.2014.47.10.286
30. Hay N, Sonenberg N. Upstream and downstream of mTOR. *Genes Dev*. 2004;18(16):1926–1945. doi:10.1101/gad.1212704
31. Hu M, Li F, Wang W. Vitexin protects dopaminergic neurons in MPTP-induced Parkinson's disease through PI3K/Akt signaling pathway. *Drug Des Devel Ther*. 2018;12:565–573. doi:10.2147/DDDT.S156920
32. Galetic I, Andjelkovic M, Meier R, Brodbeck D, Park J, Hemmings BA. Mechanism of protein kinase B activation by insulin/insulin-like growth factor-1 revealed by specific inhibitors of phosphoinositide 3-kinase–significance for diabetes and cancer. *Pharmacol Ther*. 1999;82(2–3):409–425. doi:10.1016/S0163-7258(98)00071-0
33. Zou Z, Chen J, Yang J, Bai X. Targeted Inhibition of Rictor/mTORC2 in Cancer Treatment: a New Era after Rapamycin. *Curr Cancer Drug Target*. 2016;16(4):288–304. doi:10.2174/1568009616666151113120830
34. Wu R, Chen H, Ma J, et al. c-Abl-p38α signaling plays an important role in MPTP-induced neuronal death. *Cell Death Differ*. 2016;23(3):542–552. doi:10.1038/cdd.2015.135
35. Rademacher S, Eickholt BJ. PTEN in Autism and Neurodevelopmental Disorders. *Cold Spring Harb Perspect Med*. 2019;9(11):a036780. doi:10.1101/cshperspect.a036780
36. Xu Z, Han X, Ou D, et al. Targeting PI3K/AKT/mTOR-mediated autophagy for tumor therapy. *Appl Microbiol Biotechnol*. 2020;104(2):575–587. doi:10.1007/s00253-019-10257-8
37. Sun K, Luo J, Guo J, Yao X, Jing X, Guo F. The PI3K/AKT/mTOR signaling pathway in osteoarthritis: a narrative review. *Osteoarthritis Cartilage*. 2020;28(4):400–409. doi:10.1016/j.joca.2020.02.027
38. Tong C, Wu Y, Zhang L, Yu Y. Insulin resistance, autophagy and apoptosis in patients with polycystic ovary syndrome: association with PI3K signaling pathway. *Front Endocrinol*. 2022;13:1091147. doi:10.3389/fendo.2022.1091147
39. Heras-Sandoval D, Pérez-Rojas JM, Hernández-Damián J, Pedraza-Chaverri J. The role of PI3K/AKT/mTOR pathway in the modulation of autophagy and the clearance of protein aggregates in neurodegeneration. *Cell Signal*. 2014;26(12):2694–2701. doi:10.1016/j.cellsig.2014.08.019
40. Ichimura Y, Kumanomidou T, Sou YS, et al. Structural basis for sorting mechanism of p62 in selective autophagy. *J Biol Chem*. 2008;283(33):22847–22857. doi:10.1074/jbc.M802182200
41. Li L, Tan J, Miao Y, Lei P, Zhang Q. ROS and Autophagy: interactions and Molecular Regulatory Mechanisms. *Cell Mol Neurobiol*. 2015;35(5):615–621. doi:10.1007/s10571-015-0166-x
42. Picca A, Guerra F, Calvani R, et al. Mitochondrial Dysfunction, Protein Misfolding and Neuroinflammation in Parkinson's Disease: roads to Biomarker Discovery. *Biomolecules*. 2021;11(10):1508. doi:10.3390/biom11101508
43. Bose A, Beal MF. Mitochondrial dysfunction in Parkinson's disease. *J Neurochem*. 2016;39(S1):216–231. doi:10.1111/jnc.13731
44. Kma L, Baruah TJ. The interplay of ROS and the PI3K/Akt pathway in autophagy regulation. *Biotechnol Appl Biochem*. 2022;69(1):248–264. doi:10.1002/bab.2104
45. Fan Y, He X, Chen M, Guo S, Dong Z. Pterostilbene alleviates MPTP-induced neurotoxicity by targeting neuroinflammation and oxidative stress. *Biochem Biophys Res Commun*. 2024;729:150358. doi:10.1016/j.bbrc.2024.150358
46. Prakash J, Chouhan S, Yadav SK, Westfall S, Rai SN, Singh SP. Withania somnifera alleviates parkinsonian phenotypes by inhibiting apoptotic pathways in dopaminergic neurons. *Neurochem Res*. 2014;39(12):2527–2536. doi:10.1007/s11064-014-1443-7
47. Rai SN, Yadav SK, Singh D, Singh SP. Ursolic acid attenuates oxidative stress in nigrostriatal tissue and improves neurobehavioral activity in MPTP-induced Parkinsonian mouse model. *J Chem Neuroanat*. 2016;71:41–49. doi:10.1016/j.jchemneu.2015.12.002
48. Yadav SK, Rai SN, Singh SP. Mucuna pruriens reduces inducible nitric oxide synthase expression in Parkinsonian mice model. *J Chem Neuroanat*. 2017;80:1–10. doi:10.1016/j.jchemneu.2016.11.009
49. Rai SN, Birla H, Singh SS, et al. Mucuna pruriens Protects against MPTP Intoxicated Neuroinflammation in Parkinson's Disease through NF-κB/pAKT Signaling Pathways. *Front Aging Neurosci*. 2017;9:421. doi:10.3389/fnagi.2017.00421
50. Baek SE, Jang EJ, Choi JM, Choi YW, Kim CD. α-Iso-cubebene attenuates neointima formation by inhibiting HMGB1-induced monocyte to macrophage differentiation via suppressing ROS production. *Int Immunopharmacol*. 2022;111:109121. doi:10.1016/j.intimp.2022.109121
51. Zhang C, Zhou J, Zhuo L, et al. The TLR4/NF-κB/NLRP3 and Nrf2/HO-1 pathways mediate the neuroprotective effects of alkaloids extracted from Uncaria rhynchophylla in Parkinson's disease. *J Ethnopharmacol*. 2024;333:118391. doi:10.1016/j.jep.2024.118391
52. Li T, Zhang Y, Dong R, et al. Identification and mechanistic exploration of key anti-inflammatory molecules in American ginseng: impacts on signal transducer and activator of transcription 3 STAT3 phosphorylation and macrophage polarization. *Phytother Res*. 2024;38(8):4307–4320. doi:10.1002/ptr.8277
53. Takaya K, Asou T, Kishi K. Cistanche deserticola Polysaccharide Reduces Inflammation and Aging Phenotypes in the Dermal Fibroblasts through the Activation of the NRF2/HO-1 Pathway. *Int J Mol Sci*. 2023;24(21):15704. doi:10.3390/ijms242115704
54. Zhao Q, Liu Y, Wang X, et al. Cuscuta chinensis flavonoids reducing oxidative stress of the improve sperm damage in bisphenol A exposed mice offspring. *Ecotoxicol Environ Saf*. 2023;255:114831. doi:10.1016/j.ecoenv.2023.114831
55. Gupta R, Ambasta RK, Pravir K. Autophagy and apoptosis cascade: which is more prominent in neuronal death? *Cell Mol Life Sci*. 2021;78(24):8001–8047.
56. Talebi Taheri A, Golshadi Z, Zare H, et al. The Potential of Targeting Autophagy-Related Non-coding RNAs in the Treatment of Alzheimer's and Parkinson's Diseases. *Cell Mol Neurobiol*. 2024;44(1):28. doi:10.1007/s10571-024-01461-w
57. Ullah I, Uddin S, Zhao L, Wang X, Li H. Autophagy and UPS pathway contribute to nicotine-induced protection effect in Parkinson's disease. *Exp Brain Res*. 2024;242(4):971–986. doi:10.1007/s00221-023-06765-9